

Penetrative convection of a plane turbulent wall jet in a two-layer thermally stable environment: a problem in enclosure fires

KAMLESH KAPOOR and YOGESH JALURIA

Department of Mechanical and Aerospace Engineering, Rutgers—The State University of New Jersey,
New Brunswick, NJ 08903, U.S.A.

(Received 12 June 1991 and in final form 6 February 1992)

Abstract—An experimental investigation has been carried out on the penetrative characteristics of a heated, two-dimensional, turbulent wall jet discharged downward into a two-layer thermally stable environment. Such flows, with opposing buoyancy effects, are frequently encountered in heat rejection processes and in enclosure fires. The discharge temperature of the jet is taken as higher than the upper layer temperature so that the jet is negatively buoyant in both layers. Of particular interest is the penetration of the jet into the lower layer. The conditions for which it fails to penetrate the interface between the two layers are also determined. The penetration distance of the jet is measured and related to the inflow conditions, particularly to the temperature and the velocity at the discharge. The thermal field is studied in detail to determine the basic characteristics of such flows. The mass flow rate penetrating downward as well as that rising upward due to thermal buoyancy are obtained and compared with the jet inlet mass flow rate. The heat transfer to the surface is measured for several wall temperatures and considered in terms of the penetrative flow. Flow visualization with smoke is also undertaken in order to obtain further insight into the basic nature of the flow.

INTRODUCTION

THE DISCHARGE of a buoyant jet into a stratified environment is of interest in many energy storage and heat rejection processes. Lakes, rivers and ponds are frequently stably stratified, with the temperature level decreasing as the depth increases [1]. In thermal energy storage problems, such as those of interest in solar energy storage as sensible heat, stratification usually arises in the storage tank due to the energy input [2, 3]. Similarly, at the early stages of fire growth in an enclosed region, such as a room, the heat input due to the fire generally results in the establishment of a hot upper layer above a cooler bottom layer, as studied experimentally by Zukoski [4] and Cooper *et al.* [5]. The temperature in each layer is usually fairly uniform due to thermal buoyancy and turbulent mixing and a sharp interface is often found to arise between the two. In such an environment, the plume generated by the fire impinges on the ceiling, spreads out and finally turns downward at the corners. This results in penetrative wall flows, which are of considerable interest in the modeling of enclosure fires [6, 7]. In such cases, it is important to determine the downward penetration of the wall jet, particularly whether it penetrates into the lower layer and the extent of this penetration. Also of interest are the resulting heat transfer to the wall, ambient fluid entrainment and the basic characteristics of the flow.

Turbulent buoyant jets rising in isothermal media have received considerable attention in the literature because of their importance in environmental studies

[8]. Work has also been done on the flow of laminar and turbulent buoyant jets in stratified media [9, 10]. The rise of laminar thermal plumes in a thermally stratified medium was studied by Wirtz and Chiu [11]. The downstream variations of the centerline plume velocity, temperature and plume radius were determined. They also carried out an experimental study with thermal plumes generated by small disk heaters in a thermally stratified air medium. The upward penetration of the plumes was measured for various thermal stratification levels and heat release rates. Axisymmetric jets were considered by Himasekhar and Jaluria [12]. A linear ambient temperature distribution was assumed and the temperature and velocity distributions were obtained for a wide range of governing parameters. With increasing thermal stratification, the local buoyancy level in the flow was found to reduce, as expected, resulting in a decreasing velocity level downstream. The flow was predicted to penetrate to a finite height, which was computed along with the associated reverse flow. Several other studies of flows rising in stratified environments have been reviewed by Turner [13], Jaluria [14] and Gebhart *et al.* [15]. All these flows exhibit several characteristics similar to those of a negatively buoyant jet, in which the buoyancy force is in the direction opposite to that of the flow and, thus, reduces the velocity and restricts the penetration distance of the jet.

Goldman and Jaluria [16] carried out a detailed experimental investigation of downward discharged turbulent heated air jets, in order to study the thermal and flow characteristics of two-dimensional wall and

jet in a stable thermally stratified environment. One system is needed to generate the two-dimensional heated jet and the other to establish a stable thermally stratified environment in which an essentially isothermal heated layer overlies a relatively cooler isothermal layer. The flows considered are turbulent and all the results are presented in terms of the time-averaged variables.

Figure 1 shows a sketch of the experimental arrangement employed for generating a two-layer, thermally stratified environment in a glass enclosure. Heated air flows into the enclosure over essentially the entire cross-section at the top. The inflow velocity U_d is kept small, as compared to the jet discharge velocity U_0 , and is generally of order 10 cm s^{-1} or smaller. A blower is used to force ambient air through a heated copper duct. The flow rate can be varied to obtain a desired range of flow velocity U_d at the top of the enclosure. The copper duct is 36 cm in length and $13.2 \text{ cm} \times 10.8 \text{ cm}$ in cross-section. Three fiber-glass insulated strip heaters are wrapped around it and heated electrically. The energy input to each of the heaters is varied by means of power controllers. A honeycomb and three very fine screens are used at the exit of the copper duct to ensure uniform tem-

perature and velocity distributions across the duct (see Kapoor and Jaluria [20, 21]).

The copper duct leads into a diffuser which is designed to keep the pressure loss small and the flow at the diffuser exit as uniform as possible. The diffuser has six guide vanes which divide the hot air flow from the copper duct into seven portions. These separate flows merge near the diffuser exit, where the velocity U_d is measured. The hot air is then discharged downward into the glass enclosure, which is 1.5 m high and $1.37 \text{ m} \times 0.3 \text{ m}$ in cross-section. The bottom of the enclosure is kept open in order to simulate flow in an extensive environment and to allow the lower part of the enclosure to be in contact with and be at the same temperature as ambient air. However, because of the large size of the enclosure as compared to the flow region of interest, the experimental results were found to be essentially independent of whether the bottom was open or closed. The left side of the enclosure shown in Fig. 1 is the wall adjacent to which the heated wall jet is discharged. This wall can be insulated or maintained as isothermal at a temperature of up to about 50 C above the ambient. The right side is kept open to allow the hot air to flow out. Thus, a steady flow situation is obtained, with the conditions of the

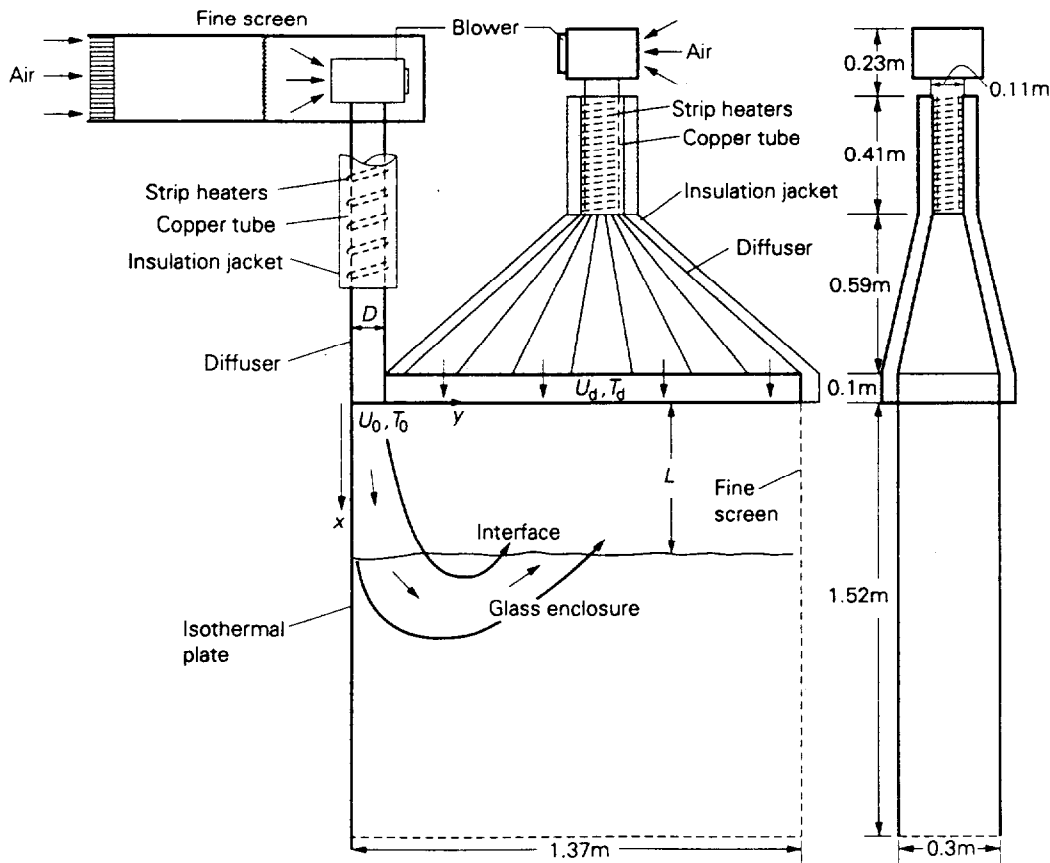


FIG. 1. Experimental arrangement for the study of the penetrative flow of a heated, two-dimensional wall jet discharged downward into a two-layer thermally stable environment.

stably stratified environment attained far from the wall over which the jet flow occurs. The remaining two, lateral, sides of the enclosure are closed by glass walls to maintain the two-dimensionality of the flow. Flow visualization is obtained by means of smoke, as outlined by Goldman and Jaluria [16].

The thermal field inside the glass enclosure is measured by means of copper–constantan thermocouples made of 7.62×10^{-5} m diameter wires, using a Keithley data acquisition system. Twenty thermocouples are fixed, at regular intervals, to the side walls of the tank. These thermocouples are used to monitor the vertical temperature distribution within the enclosure. A stably stratified, essentially two-layer, environment is generated and maintained for long periods of time by this arrangement. The stratification variables, such as the height of the interface between the two layers and the temperature levels, can be varied, as discussed in detail by Kapoor and Jaluria [21] and also outlined later in this paper. Considerable care is taken to ensure that the disturbances and velocity levels in the enclosure are very small in the absence of the wall jet. The two layers were found to be very stable, with extremely small (of order 0.5 cm s^{-1}) entrainment velocities across the interface when the jet discharge is not turned on. Also, it was ensured that the results obtained when the jet is turned on are not significantly influenced by the arrangement employed for stratifying the enclosure. For further details on these aspects, see Kapoor and Jaluria [21].

Similarly, in order to generate a two-dimensional heated wall jet, a blower is used to send ambient air, over a wide range of flow rates, through a heated copper tube. The copper tube is 5 cm in diameter and 1 m in length. It is heated by means of three fiberglass insulated heaters wrapped around it. A diffuser at the end of the copper tube is employed to discharge the heated air as a two-dimensional wall jet, whose width can be varied. Several diffuser designs were considered to ensure uniform flow at the exit. It was confirmed, by temperature and velocity measurements, that a fairly uniform, isothermal flow is obtained at the diffuser exit. A maximum difference of $\pm 5\%$ from the average values of the velocity and the temperature was obtained across the jet discharge. The thermal energy loss from the copper tube and the diffuser to the environment is reduced by employing an insulation jacket with an inner layer of fiberglass cloth tape and an outer layer of glass wool. Finally, aluminum foil is wrapped around the insulation. For further details on the arrangement, see Goldman and Jaluria [16] and Kapoor and Jaluria [20].

The discharge temperature of the jet is measured using a rake of five thermocouples located at the discharge slot. The average of the temperature measured by these five thermocouples is taken as the jet discharge temperature T_0 in the experiment. A DANTEC hot wire anemometer is employed for the measurement of discharge velocity at the jet discharge. The velocity distribution is obtained and the average

is taken as the discharge velocity U_0 . As mentioned above, the cross-stream distributions were quite uniform. Since the air temperature changes substantially in the present problem, a system for calibrating the sensor at different fluid temperatures was developed, as outlined later in the paper.

A water cooled aluminum plate, about 1 m in length, is attached to the side wall of the enclosure and the jet is discharged adjacent to this surface. Four rectangular copper channels, each $2.5 \text{ cm} \times 1.2 \text{ cm}$ in cross-section, run along the length of the plate. Water from a storage tank enters the channels at the top of the plate and the water emerging from this arrangement is allowed to drain into a sink. The temperature of the water entering the plate is maintained at a desired value by mixing hot and cold water streams from two separate sources. Nine thermocouples are embedded close to the plate surface to monitor the plate temperature. For further details on the plate assembly, see Kapoor and Jaluria [20]. The plate surface could be maintained at a constant temperature, with respect to time, by this arrangement. A fairly uniform temperature distribution was found over the plate surface, the maximum temperature difference measured between any two embedded thermocouples being of order 0.5°C .

The heat transfer from the wall jet to the plate was measured by means of microfoil heat flow sensors (RdF Type 20472-3). Each of the heat flow sensors was $1.5 \text{ mm} \times 6 \text{ mm}$ in surface area and 1 mm in thickness, and could be attached easily to the plate surface. The electric output (in mV) from the heat flow sensors yields the heat flux (in W m^{-2}) with the help of individual calibration curves, which are supplied by the manufacturer and also verified in this study by using an electrically heated surface. The accuracy of the heat flux measurements is fairly high, with an estimated error of less than 5% [20].

The velocity distribution in the flow has been obtained by means of a DANTEC constant temperature hot wire anemometer. The sensor is kept horizontal and normal to the surface when measuring the vertical component of the velocity for the two-dimensional flow under consideration. Similarly, the sensor is kept vertical for measuring the horizontal component of the velocity. The effect of the component along the sensor axis is negligible and the transverse velocity component is expected to be small for this two-dimensional flow, as also confirmed by actual measurement (see Tewari and Jaluria [22]). Though several calibration techniques are available for high velocity levels, the calibration procedure for velocity levels of less than around 1 m s^{-1} , that are expected to be encountered here, is much more difficult. The thermal plume from the hot wire sensor rises upward due to buoyancy, whereas in the present study the flow direction can be downward or upward, giving rise to opposing or aiding mixed convection flows, respectively, at the sensor. Since both the plume velocity and the flow velocity may be of the same order

of magnitude. In some cases, the calibration must be carried out in the same flow configuration as encountered in the experiment [14, 22].

A special calibration facility was developed to calibrate the hot wire anemometer for the desired velocity range, fluid temperature and flow direction. The calibration facility consists of a slide on which the hot wire is mounted. The slide is moved up and down a channel by means of a chain which is attached to an electric motor, with a speed controller. The slide can be fixed at any inclined position, from horizontal to vertical. During an experimental run, the output from the hot wire anemometer is measured by means of a Keithley data acquisition system. The output voltage is obtained from this system for different velocities and a calibration curve is plotted. Calibration curves are obtained at several air temperatures, employing the procedure, based on varying the overheat ratio of the sensor developed by Hollasch and Gebhart [23]. Using numerical methods for curve fitting and interpolation, the velocity is obtained at various locations in the flow field after correcting for the change in the local temperature from the ambient temperature. All these experimental techniques have been used earlier in other flow configurations [14, 15]. The errors in the velocity, temperature and heat flux measurements are estimated to be within 7–8% of the measured values. For further details on the calibration and on the measurement of the two velocity components, see Tewari and Jaluria [22]. The other references mentioned earlier may also be consulted for basic information on this measurement technique for small velocity levels.

The experimental results presented here are based on the measurements of the time-averaged temperature and velocity fields and of the heat transfer rates. The mean flow was found to be quite steady and the results were found to be essentially independent of the integration time for the data when this time was varied from about 20 s to a few minutes. The amplitudes of the fluctuations in the instantaneous temperature and velocity data were also measured. However, the effort was largely directed at the time-averaged quantities to indicate the important mean characteristics of the resulting transport processes. It has been mentioned earlier that the flow velocities resulting from the arrangement for generating the thermal stratification in the enclosure are negligible compared to those due to the wall jet. Another flow that arises is due to the difference between the wall and the local ambient temperatures, for the isothermal wall circumstance. This buoyancy-induced flow arises adjacent to the isothermal surface and, depending on the temperature difference, may be upward or downward in a given layer of the stratified region [7]. However, for the temperature and velocity ranges considered in this study, it can be shown that the flow rates due to these buoyancy-induced flows are in the range of 2–6% of the jet discharge flow rate. Therefore, the effect of these flows, induced by the tem-

perature difference between the wall and the ambient, on the wall jet penetrative flow under consideration is negligible. Consequently, the experimental results discussed in the next section closely represent the transport processes resulting from a wall jet penetrating into a stably stratified, two-layer, extensive environment.

EXPERIMENTAL RESULTS AND DISCUSSION

The data presented here mainly consist of measured time-averaged temperature distributions in the wall jet, local heat flux distributions along the isothermal plate for different wall temperatures, and temperature distributions in the penetrating flow. The time-averaged velocity distributions are also measured in the flow, particularly near the interface between the two layers of the stratified environment. The characteristic quantities in this transport process may be taken as the slot width D , which is appropriate since interest lies mainly in regions close to the inlet, discharge temperature T_0 , ambient temperature T_s , and discharge velocity U_0 . These lead, when the governing equations are nondimensionalized, to the dimensionless variables

$$X = \frac{x}{D}, \quad Y = \frac{y}{D}, \quad \theta = \frac{T - T_x}{T_0 - T_s}$$

$$\hat{U} = \frac{u}{U_0}, \quad \hat{V} = \frac{v}{U_0}, \quad P = \frac{p}{\rho U_0^2} \quad (1)$$

The dimensionless governing parameters obtained are

$$Re = \frac{U_0 D}{\nu}, \quad Pr = \frac{\nu}{\alpha}, \quad Gr = \frac{g\beta(T_0 - T_s)D^3}{\nu^2} \quad (2)$$

where Re , Pr and Gr are the Reynolds, Prandtl and Grashof numbers, respectively, and the other quantities are defined in the Nomenclature. Also, the Richardson number Ri , which is often employed for characterizing such flows, is defined as

$$Ri = Gr Re^2 = \frac{g\beta(T_0 - T_s)D}{U_0^2} \quad (3)$$

As mentioned later, Ri may also be based on $(T_0 - T_0)$ or $(T_0 - T_1)$, for flows within the upper or the lower layer, respectively. The upper layer temperature $\theta_u = (T_u - T_s)/(T_0 - T_s)$, the surface temperature $\theta_s = (T_s - T_s)/(T_0 - T_s)$, and the interface height L/D are three additional dimensionless parameters that arise. The local heat transfer rate is given in dimensionless form in terms of the local Nusselt number Nu_D , where

$$Nu_D = \frac{hD}{k} \quad \text{and} \quad q = h(T_0 - T_s) \quad (4)$$

Here, h is the local convective heat transfer coefficient and q the measured local heat transfer flux to the surface.

Thus, the basic governing parameters are Gr , Re ,

Pr , L/D , θ_s and θ_u . However, the fluid employed is air, so that the Prandtl number Pr is close to 0.7 for all the results presented here. The Reynolds number Re is varied from about 2×10^3 to 10^4 and the Grashof number Gr from about 10^5 to 10^7 , with a Richardson number Ri range from about 0.05 to 1.2. It has been shown in earlier papers [16, 20] that the experimental results can be very well correlated in terms of Ri and that the dependence on Re is relatively weak over the experimental range investigated. This result has also been obtained for turbulent buoyant jet flows, as reviewed by Gebhart *et al.* [15]. Therefore, the results are presented in terms of Ri in this paper, rather than in terms of the individual parameters Re and Gr .

The location of the interface, as given by the parameter L/D , is also varied, with L/D ranging from about 6.0 to 9.0. The surface temperature θ_s and the upper layer temperature θ_u are varied over wide ranges, keeping the wall jet negatively buoyant in the two regions. The slot width D is varied from 1.0 to 7.0 cm, the jet discharge temperature excess $(T_u - T_s)$ from about 10 to 80 C and the jet discharge velocity U_d from about 0.4 to 1.5 $m\ s^{-1}$. The intensity of turbulence was found to be of order 5% and the mean values, obtained by averaging over a time of more than about 20 s, are presented here. An extensive study was thus carried out. However, only some of the typical results are presented here for conciseness. These represent the general trends obtained in the study. Let us first consider the basic characteristics of the thermal stratification generated in the tank for the study of penetrative convection.

Stratification in the enclosure

Figure 2 shows the vertical temperature distributions measured within the enclosure for three different values of $\Delta T_d = T_d - T_s$, at $U_d = 0.12\ m\ s^{-1}$, where T_d and U_d are the time-averaged discharge temperature and velocity, respectively, of the heated air inflow at the top of the enclosure for stratifying the environment within it. Here $\theta_d = (T - T_s)/(T_d - T_s)$. It is seen that the temperatures are almost uniform in the upper portion of the enclosure and that a sharp decrease in the temperature level is found to arise in the region $x/H = 0.30-0.37$ at $\Delta T_d = 31.5\ C$, where H is the enclosure height. This is followed by a gradual decrease in temperature, which finally becomes equal to the ambient temperature T_s at the bottom of the enclosure. The temperature distribution obtained indicates the presence of a well established, two-layer, stably stratified environment in the enclosure. Thus, an upper hot layer of essentially uniform temperature T_u overlies a relatively cooler lower region at temperature T_l . The interface between the two layers is defined by replacing the measured temperature distribution by a step change from one zone to the other, keeping the thermal energy unchanged [21]. This yields the value of the parameter L/D that characterizes the location of the interface in later experiments. As mentioned earlier, the fluctuations in vel-

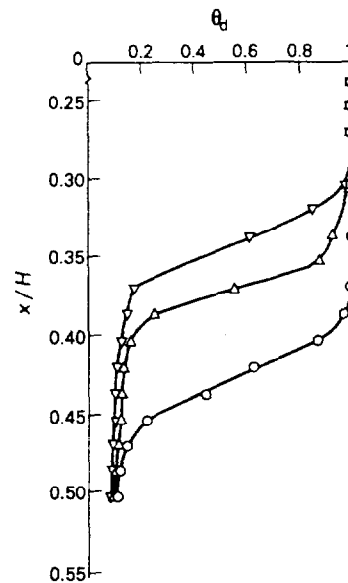


FIG. 2. Effect of the discharge temperature difference $\Delta T_d = T_d - T_s$ on the stratification in the enclosure at $U_d = 0.12\ m\ s^{-1}$ and $T_s = 26.0\ C$. (∇) $\Delta T_d = 31.5\ C$; (Δ) $\Delta T_d = 23.0\ C$; (\circ) $\Delta T_d = 13.5\ C$.

ocity and temperature were found to be extremely small in the vicinity of the interface in the absence of the wall jet and also far from the wall when the jet flow was present. An estimate of the turbulent energy flux across the interface for these circumstances indicated it to be negligible compared to the thermal diffusion effect, which is also the main cause for the temperature spread near the interface.

It was found that the temperature distribution remains essentially constant with time and thus could be maintained indefinitely. As can be seen from the figure, the location of the interface moves upward as ΔT_d is increased. Time-averaged velocity data were also obtained in the enclosure. It was found that the mean velocities were largely in the range of 0-3 $cm\ s^{-1}$ for the flow rates employed here, except very near the inlet. The presence of such low velocity levels indicates that the upper hot layer is fairly stagnant in nature and that the effect of these velocities on the flow under consideration may be neglected. Also, due to the strong thermal stratification obtained, the entrainment from the lower to the upper layer, across the interface, was found to be negligible. Several other results similar to those shown in Fig. 2 were obtained by Kapoor and Jaluria [21]. The inlet conditions needed for the desired interface location and temperature levels for the two-layer environment in the enclosure may be determined, employing results on the dependence of L/H on the discharge conditions for stratifying the tank, as represented by the Richardson number Ri_d , where $Ri_d = g\beta(T_d - T_s)H/U_d^2$. Therefore, the interface location may be varied by a proper choice of T_d and U_d [21].

Jet penetration into a two-layer stably stratified environment

The variation of the penetration distance δ_p with the mixed convection parameter Ri , for an adiabatic condition at the vertical surface, is shown in Fig. 3. The penetration depth δ_p was defined as the vertical distance, from the jet discharge, over which significant thermal effects are observed. In most cases, it was found to be close to the vertical location where the local maximum temperature excess ($T_{max} - T_x$) has dropped to 1% of inlet excess temperature, ($T_0 - T_x$) (see Goldman and Jaluria [16]). A horizontal array of thermocouples was moved upward through the lower zone, toward the interface, till a sharp increase in the temperature level was observed. This location was obtained quantitatively by plotting the vertical temperature distributions in the flow and taking a sharp change in the profiles as indicative of the extent of the downward penetration of the thermal field. It was found that the repeatability of this measurement was high, being within about 5% of the measured penetration distance. The choice of an arbitrary criterion, such as ($T_{max} - T_x$) being 1% of ($T_0 - T_x$), for obtaining δ_p was found to yield poor repeatability and also inaccuracy in measurement because of the relatively gradual vertical temperature variation in much of the region far from the jet discharge. However, a sharp change in the profile was clearly observed downstream and was used to define the downward penetration distance δ_p . This location also agreed with the flow visualization results, as shown by Goldman and Jaluria [16] and also discussed later in this paper.

It is seen from Fig. 3 that, at a given value of Ri , the jet penetrates to a much larger distance in the stratified environment than in an isothermal one at the ambient temperature of T_x . This is because of a smaller opposing buoyancy effect in the former case. The buoyancy force is governed by the temperature difference ($T_0 - T_a$), where T_a is the local environ-

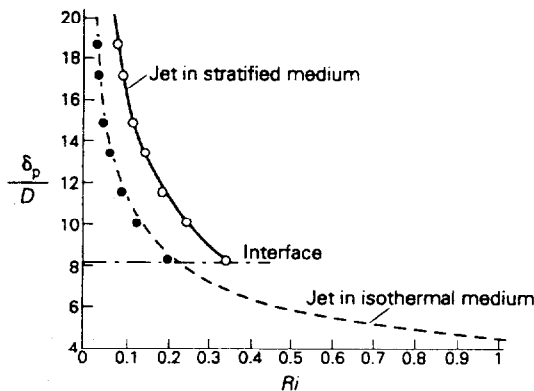


FIG. 3. Measured penetration depth δ_p for a negatively buoyant jet adjacent to an adiabatic wall in an isothermal medium, as well as that in a stably stratified two-layer environment, for $T_0 - T_1 = 33$ C, $T_x = 25$ C and $L/D = 8.2$. (●) Ri based on $T_0 - T_u$; (○) Ri based on $T_0 - T_x$, taking $T_l = T_x$; (---) jet in an isothermal environment.

mental temperature. Thus, T_a is the lower layer temperature T_l or the upper layer temperature T_u , depending on the zone under consideration. The opposing buoyancy force is much larger in the lower zone than in the upper layer. Similarly, the buoyancy effect in an isothermal environment at T_x or T_l is much larger than that in the upper zone at T_u . This results in a smaller penetration depth in an isothermal region at T_x .

It is interesting to note that if the mixed convection parameter Ri is defined in terms of ($T_0 - T_u$), which is the jet discharge temperature excess over the upper layer temperature T_u (see equation (3)), the dimensionless results are found to be close to those for a jet in an isothermal medium, whose temperature is now taken as T_u since Ri is defined in terms of this temperature. This is due to the fact that, as mentioned earlier, the buoyancy effect in the jet is determined by the temperature difference ($T_0 - T_u$) in the upper zone, which plays a dominant role in determining the penetration of the jet in the two-layer environment. Thus, by defining Gr in terms of ($T_0 - T_u$), the buoyancy effect in the upper zone is accounted for. However, the penetration distance δ_p is found to be smaller in the stratified case than in an isothermal medium at temperature T_u . This is an expected result, since in the former circumstance, the flow encounters an increased opposing buoyancy force as it penetrates into the lower layer, a situation that does not arise in the isothermal medium.

The measurements of the penetration distance can be correlated in terms of the δ_p/D dependence on Ri , which is the dominant parameter that affects penetration [16, 20]. The correlating equations thus obtained for the parametric range shown in Fig. 3, for an insulated vertical surface, are

$$\frac{\delta_p}{D} = 4.45(Ri)^{-0.405}, \quad Ri \text{ based on } (T_0 - T_u) \quad (5)$$

$$\frac{\delta_p}{D} = 4.45(Ri)^{-0.576}, \quad Ri \text{ based on } (T_0 - T_x) \quad (6)$$

$$\frac{\delta_p}{D} = 4.45(Ri)^{-0.410}, \quad \text{for an isothermal medium.} \quad (7)$$

The correlation coefficients, which characterize the accuracy of the representation of the data with a correlating equation [24], for all these results were calculated and were found to be around 0.99. Thus, these correlating equations closely approximate the data obtained.

It must be noted that the results presented in Fig. 3 were for $L/D = 8.2$ and the given temperature levels in the stratified region. The penetration depth δ_p is obviously a function of L/D , θ_w and the thermal conditions at the wall. The value of L/D determines if the flow penetrates into the lower layer. If δ_p from equation (7) is less than L , the flow is contained within an isothermal region at temperature T_u and the results obtained by Goldman and Jaluria [16] and Kapoor

and Jaluria [20] may be employed to characterize the flow. Therefore, this situation applies if $4.45(Ri)^{-0.41} < L/D$, where Ri is based on $(T_w - T_w)$. However, if the flow penetrates into the lower layer, both θ_w and L/D become important parameters in characterizing the flow and the penetration. For the range of L/D considered here, the results, in dimensionless form, were found to vary weakly with L/D . However, for very small values of L/D , the dependence of the penetration on L/D is expected to be much stronger. The effect of the temperature distribution is included in the results through the Richardson number and that of the surface temperature is considered below.

Penetration depth measurements were also made for the isothermal surface condition. The corresponding heat transfer results are discussed later in the paper. The physical characteristics of the penetrative flow were very similar to those obtained earlier for the adiabatic thermal condition at the wall, though the actual measured value of δ_p was altered, as expected. Due to heat transfer to the wall, the opposing buoyancy effect is reduced, resulting in larger penetration distances compared to those for the adiabatic condition. This trend was also observed by Kapoor and Jaluria [20] for negatively buoyant wall jets in extensive, isothermal media. The penetration distance δ_p measured in the present study was closely correlated by the equation

$$\frac{\delta_p}{D} = (4.1 - 5.9\theta_w)(Ri)^{-0.4 + 0.9\theta_w} \quad (8)$$

for θ_w ranging from 0.0 to 0.5. Here, $\theta_w = (T_w - T_s)/(T_w - T_s)$, T_s being the surface temperature and T_s the ambient temperature, as defined earlier in equation (1). Therefore, the penetration depth δ_p is increased due to heat loss to the wall and a smaller value of θ_w leads to a larger penetration distance.

The location of the interface between the two layers, as obtained by replacing the measured temperature distribution by an idealized two-layer region with the same thermal energy, is also shown in Fig. 3. The results shown here are restricted to a maximum Ri value of about 0.35, since for larger values of Ri the jet flow was found to be contained within the upper layer only and unable to penetrate into the lower layer, for the chosen thermal stratification of the environment. Thus, for $Ri > 0.35$, the problem reduces to that of a negatively buoyant jet in an isothermal medium at temperature T_w . As discussed above, the results obtained in earlier studies may thus be used to determine the characteristics of the flow for $Ri \leq 0.35$.

In order to obtain a better understanding of the basic nature of the penetrative wall jet flow, a detailed measurement of the thermal field was also carried out, using an array of thermocouples. Typical measured time-averaged temperature distributions are shown in Fig. 4 at $Ri = 0.1$. All these measurements were taken

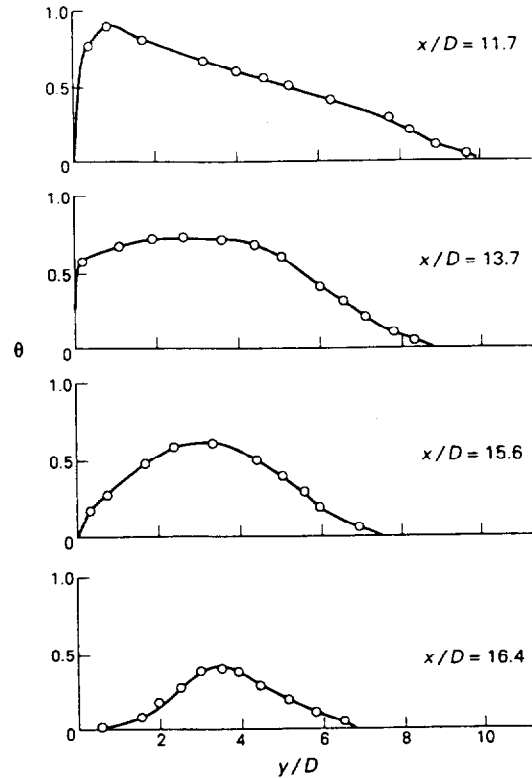


FIG. 4. Measured temperature profiles at various vertical locations below the interface, which is at $x/D = 8.8$. For $Ri = 0.1$, $T_w - T_s = 33$ C ($\theta_w = 0.62$) and $\theta_s = 0.0$.

below the interface, which was at $x/D = 8.8$ for this experiment. Thus, a decrease in the temperature level as x increases and an outward spread of the thermal field, indicating the shift from the downward wall flow to the upward reverse flow, are clearly seen. From these measurements, the corresponding time-averaged isotherms may be obtained by interpolation, as shown in Fig. 5. The isotherms indicate the thermal field resulting from the penetration of the wall jet across the interface for the conditions indicated. The basic characteristics of this flow in the lower zone, following penetration, are very similar to those of a negatively buoyant jet in an isothermal medium (see Turner [13, 17]). Thus, the penetration in the lower layer may be characterized in terms of a local Richardson number at the interface. The fluid in this flow penetrates to a finite vertical distance, becomes stationary and then rises vertically upward due to thermal buoyancy as a plume. A large outward spread of the flow, away from the wall, is seen. This is in agreement with the earlier work of Goldman and Jaluria [16] and of Kapoor and Jaluria [20], who observed a large horizontal spread of the flow and also obtained a large entrainment into the flow for Ri values ranging up to about 0.6.

Flow field near the interface

The penetration of the wall jet across the interface affects the transport between the two layers. In the

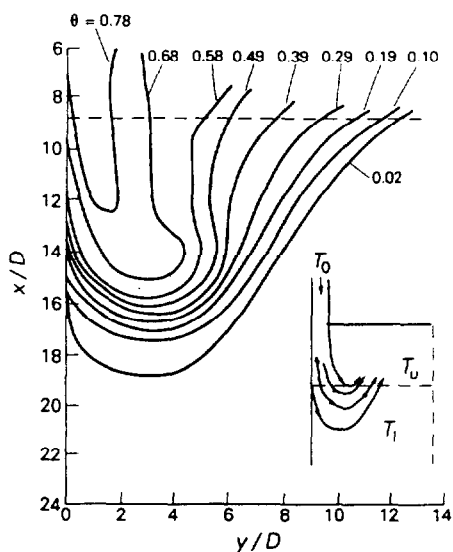


FIG. 5. The thermal field, in terms of the isotherm distribution, resulting from the penetration of a negatively buoyant wall jet into the lower layer of a two-layer stably stratified medium for the conditions of Fig. 4.

relevant problems of practical interest, mentioned earlier, it is important to study the flow field near the interface and to estimate the flow rate which penetrates into the lower layer as well as that which rises upward across the interface [6, 7]. In order to estimate these flow rates, it is necessary to measure the distribution of the time-averaged vertical velocity component in the vicinity of the interface. As mentioned earlier, a constant temperature hot wire anemometer was used for the velocity measurements in this study. The hot wire sensor was kept horizontal and perpendicular to the surface. For the two-dimensional flow under consideration, the transverse velocity component is negligible, as was also confirmed from actual measurement. These measurements yield the velocity component normal to the sensor, this being the vertical component of the flow velocity. The hot wire was also employed in other flow orientations, using the flow in a channel which could be inclined to confirm the accuracy of these measurements. For further details on the calibration and on these measurements, see Tewari and Jaluria [22].

A typical vertical time-averaged velocity distribution obtained from the measurements is shown in Fig. 6(a) at $Ri = 0.121$ and at $x/D = 8.8$, which corresponds to the location of the interface between the two layers. It is seen that, as one moves away from the surface, the velocity increases from zero at the wall to a fairly uniform value in the downward flow. It then gradually decreases along the y direction, away from the wall, becomes zero and then negative. A negative value here represents an upward flow. This upward flow velocity increases up to a certain distance from the wall and then decreases gradually to finally

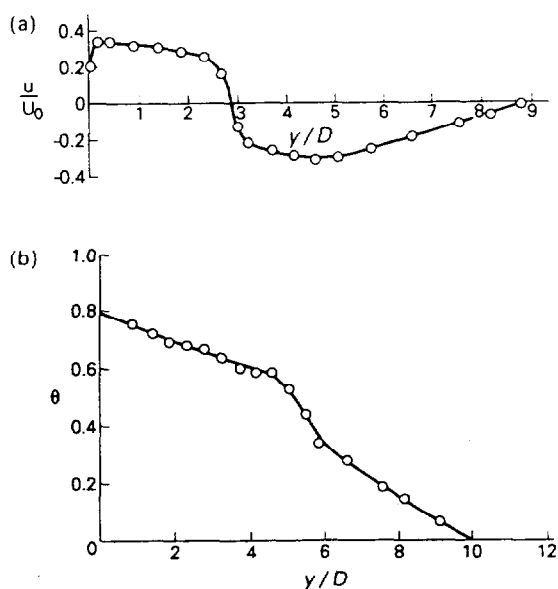


FIG. 6. Measured distributions of the vertical velocity component (a) and temperature (b) at the interface ($L/D = 8.8$) of the idealized two-layer environment at $Ri = 0.121$, $T_0 - T_1 = 33$ C ($\theta_0 = 0.51$) and $\theta_s = 0.0$.

become zero far from the wall, as expected. It is interesting to note that the region of downward flow has increased in dimensionless thickness from 1.0 at $x = 0$ to about 2.8 at this vertical location. The upward flow also has a much greater horizontal extent, as observed in earlier studies [16]. The velocity levels have clearly decreased substantially from 1.0 at the discharge to account for this large horizontal spread. The basic trends indicated by this figure are, therefore, physically expected.

The corresponding time-averaged temperature distribution at this vertical location is shown in Fig. 6(b). As can be seen from this figure, the temperature decreases gradually in the y direction, starting with a maximum value at the wall, and finally becomes equal to that of the local surroundings. A relatively sharp change in the temperature level arises between the downward and upward flow streams. Clearly, the thermal energy diffuses outward rapidly as the flow proceeds downstream. By integrating the product of the local time-averaged velocity and the density, as obtained from the measured temperature distribution, over the distance from the wall, mass flow rates can be obtained for both the downward and the upward flows. Several measurements such as those shown in Fig. 6 were taken and trends similar to those discussed above were obtained over the experimental range considered here.

The jet mass flow rate, m_j , discharged at the slot is given per unit transverse dimension by the expression

$$m_j = \rho_0 D U_0 \quad (9)$$

where ρ_0 is the air density at the jet discharge temperature. This mass flow rate is employed in non-

dimensionalizing the time-averaged penetrative mass flow rates. The mass flow rate which penetrates downward across the interface m_p was computed from the measured velocity and temperature distributions and compared with the jet discharge mass flow rate m_j . The variation of m_p/m_j with Ri is shown in Fig. 7(a). It is seen that for small values of Ri , corresponding to small jet excess temperatures $(T_0 - T_s)$ for given D and U_0 , the penetrating mass flow rate is close to the discharged mass flow rate. However, at higher values of Ri , for which the jet excess temperature $(T_0 - T_s)$ is larger, resulting in a larger opposing buoyancy force, the penetrative mass flow rate is found to be less than the discharged jet mass flow rate. This indicates that for larger values of Ri , the jet loses a larger portion of the flow in the upper layer. The opposing buoyancy effect is stronger at larger values of Ri , resulting in a shorter penetration distance, as seen earlier. Flow reversal occurs over the entire length of the wall jet, particularly in the outer region of the jet, as seen in Fig. 5, and this effect is expected to increase as Ri is increased. The results in Fig. 7(a) confirm this trend. In fact, for $4.45 Ri^{-0.41} < L/D$, with Ri based

on $(T_0 - T_s)$, m_p becomes zero, since the wall jet does not penetrate into the lower layer, as seen earlier.

Figure 7(b) shows the variation of m_0/m_p with Ri , where m_0 is the time-averaged buoyant mass flow rate rising upward to enter into the upper layer, as sketched in the figure. It is seen that at small values of Ri , the mass flow rising upward is 3–4 times the downward, penetrating mass flow. This implies that the downward, penetrating jet flow entrains a substantial amount of fluid from the lower layer. Similar trends have been seen in earlier studies [16, 20]. The entrainment is found to decrease with an increase in Ri . This may be explained as follows. With increasing Ri , the opposing buoyancy effect increases and the penetration distance δ_p decreases. As $Ri \rightarrow 0$, the upward flow becomes weaker for the isothermal wall condition because of the heat transfer to the wall. As this parameter increases from zero, the upward flow becomes more vigorous and the mass flow rate increases. However, due to the decrease in penetration distance with increasing values of Ri , the entrainment into the flow is expected to decrease at large Ri . Again, for $4.45 Ri^{-0.41} < L/D$, employing Ri based on the upper layer temperature difference $(T_0 - T_u)$, m_0 becomes zero since the wall jet does not penetrate into the lower layer. There are clearly two opposing effects acting here. With increasing Ri , the penetration distance decreases and the upward buoyant flow increases in strength. The first effect decreases the total entrainment into the negatively buoyant flow and the latter effect increases it. It is seen from Fig. 7(b) that, over the investigated range, the former effect dominates. The values of the parameter Ri shown in Fig. 7(b) are based on the inlet conditions of the jet. However, a local value of Ri can also be defined in terms of the conditions at the interface, as mentioned earlier. These local values are in the range of 1.0–4.5 for the data shown in Fig. 7(b), indicating a large opposing buoyancy effect in the lower region and the consequent decrease in entrainment with an increase in this parameter.

Heat transfer to an isothermal surface

The local surface heat flux q , varying along the height of the isothermal plate due to the discharge of the heated jet adjacent to it, was measured. The heat transfer rate may be expressed in terms of the Nusselt number, Nu_D , based on the width D of the slot through which the jet is discharged, as defined in equation (4). The distribution of the Nusselt number $Nu_D = hD/k$ along the isothermal plate, for $Ri = 0.148$ and three values of the plate temperature θ_s , is shown in Fig. 8(a). Here, $h = q/(T_0 - T_s)$, as mentioned earlier. The corresponding penetration distances δ_p have also been marked in the figure. It is seen that the local heat transfer rate decreases sharply along the plate height and then becomes essentially uniform over the remaining portion of the plate. Thus, for a dimensionless surface temperature θ_s of -0.008 , which represents the case of $T_s \approx T_s$, the local heat transfer to the plate

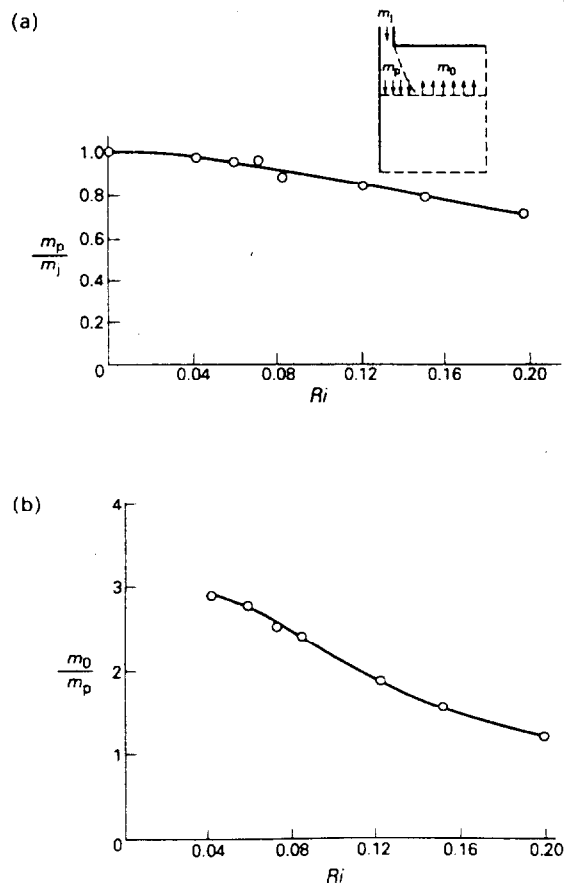


FIG. 7. Variation of the downward penetrative mass flow rate m_p across the interface (a) and ratio of the upward, buoyant flow rate m_0 to m_p at the interface (b) with Ri at $T_0 - T_s = 33$ C, $\theta_s = 0.0$ and $L/D = 8.75$.

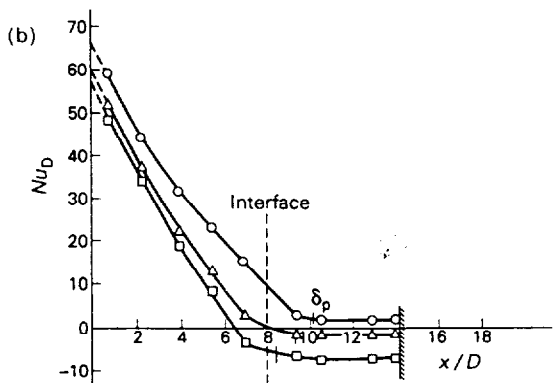
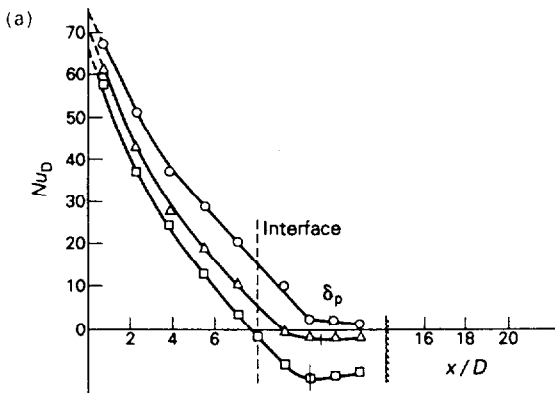


FIG. 8. Local heat transfer rate to the wall, given in terms of the local Nusselt number Nu_D , in a two-layer stably stratified environment. (a) $Ri = 0.148$, $T_u - T_l = 35$ C ($\theta_u = 0.66$) and $L/D = 8.0$: (\circ) $\theta_p = -0.008$; (\triangle) $\theta_p = 0.2$; (\square) $\theta_p = 0.4$. (b) $Ri = 0.249$, $T_u - T_l = 35$ C ($\theta_u = 0.39$) and $L/D = 8.0$: (\circ) $\theta_p = -0.005$; (\triangle) $\theta_p = 0.12$; (\square) $\theta_p = 0.23$.

does not become zero even after the jet reverses its direction. This is due to the fact that the ambient temperature T_a , which is 25 C for this experiment, is slightly higher than the plate temperature T_p .

The results for plate temperature θ_p values of 0.2 and 0.4 are similar to that observed for the plate temperature θ_p of -0.008 , except that the heat transfer rate becomes negative after a certain distance, indicating heat loss by the plate to the environment. The distance over which q is positive is denoted as δ_H and is found to be the distance up to the location where the local jet temperature becomes essentially equal to the plate temperature T_p . The temperature level in the jet flow, from δ_H to δ_p , is therefore lower than the plate temperature. Obviously, heat is transferred from the isothermal plate to the jet in this region. Figure 8(b) shows the corresponding results at a different value of the Richardson number Ri . Trends very similar to those seen in Fig. 8(a) are observed. The penetration distances are smaller due to the larger Ri , as compared to the corresponding values in Fig. 8(a).

The decay of the temperature level with the height is seen more clearly in Fig. 9, which shows the local maximum temperature in the wall jet flow as a func-

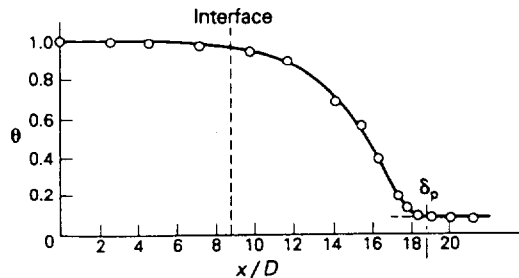


FIG. 9. The downstream decay of the maximum temperature in the flow at $Ri = 0.08$, $T_u - T_l = 33$ C ($\theta_u = 0.62$) and $\theta_p = 0.0$.

tion of the height x . The observed trends support the measured heat transfer rate variation over the vertical surface. This figure also shows the sharp change in the temperature distribution that is used for the determination of δ_p . Clearly, the penetration of thermal effects is indicated by a sharp deviation from the uniform or gradually varying temperature distribution far downstream. Similar trends were observed at other values of the governing parameters.

Flow visualization

The flow was also visualized with smoke. The smoke is generated by the evaporation of kerosene oil as it flows through an electrically heated steel tube. The smoke was introduced into the flow upstream of the diffuser so that it becomes heated along with the air and exits at the same local temperature as the jet. Figure 10 shows photographs of the movement of smoke introduced into the steady penetrative flow under investigation. Figures 10(a) and (b) show the basic flow characteristics of a wall jet penetrating into a two-layer stably stratified environment. Figure 10(c) shows the smoke moving out of the enclosure. These pictures confirm the existence of a well established hot upper layer, at an essentially uniform temperature, inside the enclosure and qualitatively indicate the wall jet penetration into the lower layer. A fairly sharp interface is seen, as discussed earlier. The jet flow penetrates across the interface, entrains fluid from the lower isothermal layer and finally escapes through the open end of the enclosure. The penetration distance δ_p is clearly defined. These observations agree with the detailed measurements of the temperature and velocity distributions discussed earlier. It is also observed that the stratified environment away from the wall jet remains essentially unaffected by the flow, lending support to the experimental procedure employed here to study the penetration of a wall jet.

The visualization procedure was also extended to various other circumstances, such as the situation when the wall jet fails to penetrate with the lower layer and is contained within the upper region. Results similar to those presented by Goldman and Jaluria [16] were obtained in this case. Similarly, the differ-

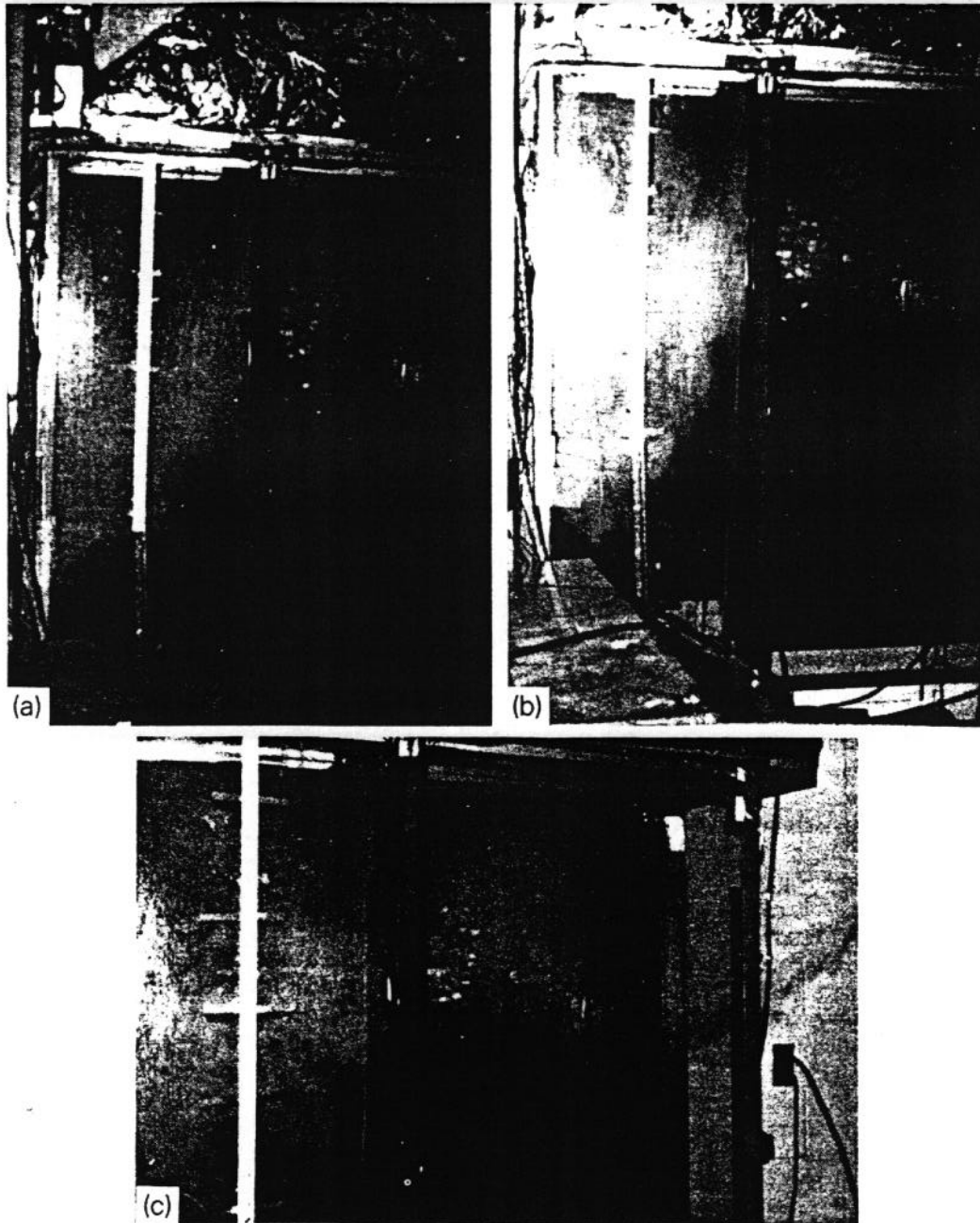


FIG. 10. Photographs indicating the flow of smoke in the penetration of a two-dimensional wall jet into the lower layer of a two-layer thermally stable environment.

ence in the flow penetration for isothermal and adiabatic wall conditions was investigated, confirming that the penetration distance is larger in the latter case. Thus, visualization may be employed to provide qualitative corroboration of the experimental results in such penetrative flows.

CONCLUSIONS

A detailed experimental study has been carried out to investigate the interesting flow circumstance of a heated, downward discharged wall jet in a two-layer thermally stable environment, when the jet is negatively buoyant in both the layers. The penetrative

jet flow in such thermally stratified environments is important in many practical problems, such as enclosure fires and thermal energy discharge into the environment. A heated two-dimensional jet at temperature T_0 is discharged vertically downward adjacent to an adiabatic or isothermal plate in a large enclosure. The penetration distance δ_p was measured and was found to be greater than that in an isothermal medium at the lower layer temperature. This is due to the fact that the opposing buoyancy effect, which depends upon the difference between the jet discharge temperature and the local ambient temperature, is much smaller in the upper zone, which is at a tem-

perature higher than that of the lower layer for a stable stratification. However, if the buoyancy parameter Ri is defined in terms of the upper layer temperature T_u , the nondimensional results are found to be close to those for a negatively buoyant jet in an isothermal medium at the upper layer temperature T_u . This implies that the buoyancy effect resulting from the temperature difference ($T_u - T_o$) in the upper layer is the dominant mechanism in this penetrative flow over the experimental range investigated. Correlating equations are also obtained for estimating δ_p for a wide range of operating conditions.

A detailed study of the resulting thermal and flow fields has also been carried out. The results are presented in terms of the time-averaged variables and show that the flow characteristics following penetration into the lower region are very similar to those for a negatively buoyant jet in an extensive, isothermal medium. The mass flow rate which penetrates downward, across the interface, and the mass flow rate which rises upward due to buoyancy are determined from the velocity and temperature distributions measured close to the interface. For large values of Ri , the jet loses a significant portion of the fluid flow from the discharge location up to the interface, due to the opposing buoyancy effects, and is found not to penetrate at all if the Richardson number is large enough to restrict the penetration to the interface location. Following the penetration, if the flow does penetrate, the flow entrains fluid from the lower layer. The local heat transfer flux measurements along the length of the isothermal plate show that the local heat transfer rate decreases sharply along the plate, becoming fairly small beyond the penetration distance and gradually decaying to zero far downstream. The heat transfer rate to the plate beyond $x = \delta_p$ is positive, zero or negative, depending on whether the plate temperature T_s is smaller than, equal to or larger than the ambient temperature T_a . Again, correlating equations are derived from the experimental data to allow an estimate of the heat transfer rate to the surface. The flow circumstance considered is a complicated, though important, one and this study presents a detailed study of the basic transport processes involved and also yields quantitative information on physical quantities of interest in several practical problems, particularly those related to enclosure fires.

Acknowledgements—This research was carried out with support from the Center for Fire Research of the National Institute of Standards and Technology, United States Department of Commerce, under Grant number 60NANB7D0743. The several helpful suggestions of Dr L. Y. Cooper during the course of this work are also acknowledged.

REFERENCES

1. F. K. Moore and Y. Jaluria, Thermal effects of power plants on lakes. *J. Heat Transfer* **94**, 163–168 (1972).
2. T. D. Brumleve, Sensible heat storage in liquids. Sandia National Laboratories, Livermore, GA, SLL-73-0263 (1974).
3. S. K. Gupta and Y. Jaluria, An experimental and analytical study of thermal stratification in an enclosed water region due to thermal energy discharge. *Energy Conv.* **22**, 63–70 (1982).
4. E. E. Zukoski, Development of a stratified ceiling layer in the early stages of a closed room fire. *Fire Materials* **2**, 54–62 (1978).
5. L. Y. Cooper, M. Harkleroad, J. Quintiere and W. Rinkinen, An experimental study of upper hot layer stratification in full-scale multiroom fire scenario. *J. Heat Transfer* **104**, 741–749 (1982).
6. L. Y. Cooper, On the significance of a wall effect in enclosure with growing fires. *Combust. Sci. Technol.* **40**, 19–39 (1984).
7. Y. Jaluria, Buoyancy driven wall flows in enclosure fires. *Proc. 21st Symp. (Int.) on Combustion*, Combust. Inst., Pittsburgh, Pennsylvania, pp. 151–157 (1986).
8. E. J. List, Turbulent jets and plumes. *Ann. Rev. Fluid Mech.* **14**, 189–212 (1982).
9. R. B. Darden, J. Imberger and H. B. Fisher, Jet discharge into a stratified reservoir. *ASCE, J. Hyd. Div.* **101**, 1211–1220 (1975).
10. A. R. Tenner and B. Gebhart, Laminar and axisymmetric vertical jets in a stably stratified environment. *Int. J. Heat Mass Transfer* **14**, 2051–2062 (1971).
11. R. A. Wirtz and C. M. Chiu, Laminar thermal plume rise in a thermally stratified environment. *Int. J. Heat Mass Transfer* **17**, 323–329 (1974).
12. K. Himasekhar and Y. Jaluria, Laminar buoyancy-induced axisymmetric free boundary flows in a thermally stratified medium. *Int. J. Heat Mass Transfer* **25**, 213–221 (1982).
13. J. S. Turner, *Buoyancy Effects in Fluids*. Cambridge University Press, London (1973).
14. Y. Jaluria, *Natural Convection Heat and Mass Transfer*. Pergamon Press, Oxford (1980).
15. B. Gebhart, Y. Jaluria, R. L. Mahajan and B. Sammakia, *Buoyancy-Induced Flows and Transport*. Hemisphere, New York (1988).
16. D. Goldman and Y. Jaluria, Effect of opposing buoyancy on the flow in free and wall jets. *J. Fluid Mech.* **166**, 41–56 (1986).
17. J. S. Turner, Jets and plumes with negative or reversing buoyancy. *J. Fluid Mech.* **27**, 779–792 (1966).
18. R. A. Seban, M. M. Behnia and J. E. Abreu, Temperatures in a heated jet discharged downward. *Int. J. Heat Mass Transfer* **21**, 1453–1458 (1978).
19. Y. Jaluria and K. Kapoor, Importance of wall flows at the early stages of fire growth in the mathematical modelling of enclosure fires. *Combust. Sci. Technol.* **59**, 355–369 (1988).
20. K. Kapoor and Y. Jaluria, Heat transfer from a negatively buoyant wall jet. *Int. J. Heat Mass Transfer* **32**, 697–709 (1989).
21. K. Kapoor and Y. Jaluria, An experimental study of the generation and characteristics of a two layer thermally stable environment. *Int. Commun. Heat Mass Transfer* **15**, 751–764 (1988).
22. S. S. Tewari and Y. Jaluria, Calibration of constant-temperature hot-wire anemometers for very low velocities in air. *Rev. Scient. Instrum.* **61**, 3834–3845 (1990).
23. K. Hollasch and B. Gebhart, Calibration of constant temperature hot-wire anemometers at low velocities in water with variable fluid temperature. *J. Heat Transfer* **94**, 17–22 (1972).
24. Y. Jaluria, *Computer Methods for Engineering*. Prentice-Hall, Englewood Cliffs, New Jersey (1988).